1.55 μm DFB Laser with ns-level pulses for LiDAR

Te-Hua Liu[1,2], Hong-Ye Lin[3], Hao-Tien Cheng[2,3], and Chao-Hsin Wu[1,2,3,4,*]

[1]Graduate School of Advanced Technology, National Taiwan University, Taipei 10617, Taiwan
[2]Center for Quantum Science and Engineering, National Taiwan University, Taipei 10617, Taiwan
[3]Graduate Institute of Electronics Engineering, National Taiwan University, Taipei 10617, Taiwan
[4]Graduate Institute of Photonics and Optoelectronics, National Taiwan University, Taipei 10617, Taiwan
[*]Corresponding e-mail: chaohsinwu@ntu.edu.tw

Keywords: DFB laser, LiDAR, short-pulsed operation

Abstract

Our team has successfully manufactured a high-power, highly wavelength-stable 1.55 μm BHDFB laser. This laser has a threshold current below 15 mA, with a differential slope far surpassing the industry standard at 0.30 W/A. To mitigate thermal roll-off and improve the performance of the laser, we have incorporated the application of ns-level instantaneous voltages into the laser. This innovation has increased pulse optical power by over 50 times, enabling the DFB laser diode to produce an impressive power output in excess of 5W. Given its eye-safe design, exceptional stability, and high operational efficiency, the DFB laser we have developed is highly suitable for use in the rapidly growing field of autonomous vehicles. It provides a combination of performance, safety, and reliability, making it an ideal option for demanding applications in the LiDAR field.

INTRODUCTION

Recently, there has been a growing focus on developing light sources for detection in LiDAR systems due to the increasing importance of autonomous driving systems in the industry [1-2]. Achieving a reasonable detection distance and image resolution requires laser diodes capable of outputting watt-level optical power and stable spectral characteristics. The Fabry-Perot (FP) LD remains the typical structure for the light source in LiDAR systems due to its high optical output and low production cost. However, the wavelength redshift of FP LDs often exceeds tens of nanometers, requiring LiDAR system receivers to have a sizeable spectral bandwidth bandpass filter. To address this issue, distributed feedback (DFB) lasers have emerged as an excellent alternative. With excellent wavelength stability and high operating power, DFB lasers are well-suited for use in time-of-flight (ToF) and frequency-modulated continuous waves (FMCW) [3-4]. ToF can detect longer distances, while FMCW can obtain more mapping information despite its shorter detection range.
Moreover, we designed our laser wavelength at 1.55 μm to prevent harm to the human eye during pulsed operation, as opposed to the traditional 905 nm band used by laser manufacturers [5]. Our research also introduced a buried heterostructure (BH) to optimize the leakage current of LD issues during high-current operation and achieve high operational efficiency. BHDFB lasers based on an n-side grating can have lower diode resistance and threshold current [6]. Finally, we utilized a commercial short pulse driver to introduce ns-level pulse width, allowing the laser to operate at low pulse widths and achieve watt-level optical power.

THE DESIGN AND FABRICATION OF THE BHDFB LASER

InGaAsP material can be utilized as the active layer and can be paired with both the BH structure and the n-buried grating. The absence of Al in the material results in the regrowth stage of producing the BH structure, not having any additional defects, thereby preventing the degradation of the laser's operational characteristics. The DFB laser emission wavelength is designed at 1.55 μm. The n-buried grating is created by alternating InGaAsP and InP, with a grating structure period of 242 nm, allowing the Bragg wavelength to be matched with the gain wavelength of the laser. The active region width of the laser diode is defined to be 2 μm through an etching process. The BH structure uses a p/n/p doped electron-blocking layer to fill and wrap around the laser's active region. Finally, the DFB laser resonant cavity length is 1000 μm, and the reflective surface coating is completed after dicing.

Due to the LD's eventual connection to an external circuit board, the 1.55 μm DFB laser is packaged into the TO-56 form factor, as shown in Fig. 1(a). Additionally, compared to the commonly used COB packaging technology, a TO-CAN package can reduce the phenomenon of thermal accumulation in the laser. When the laser operates at high voltage injection with short pulses, it can reduce power degradation.

THE OPTOELECTRICAL CHARACTERISTICS OF DFB LASER

Fig. 1(b) illustrates the light-current-voltage (L-I-V) curve of the encapsulated 1.55 μm BHDFB laser under room temperature conditions. Thanks to the advancement in encapsulation technology, more than 80% of the laser chip's optical intensity can be transmitted through the lens. A high-precision IV analyzer provided the current to measure the optical and electrical characteristics of the DFB laser under

CW operation. The results show that the threshold current was below 15 mA, and the differential efficiency exceeded 0.35. It can be observed that the threshold current was only 12 mA, and the differential slope was more significant than 0.30 W/A. The output light power reached 87.44 mW, and the diode resistance was only 4 ohms.

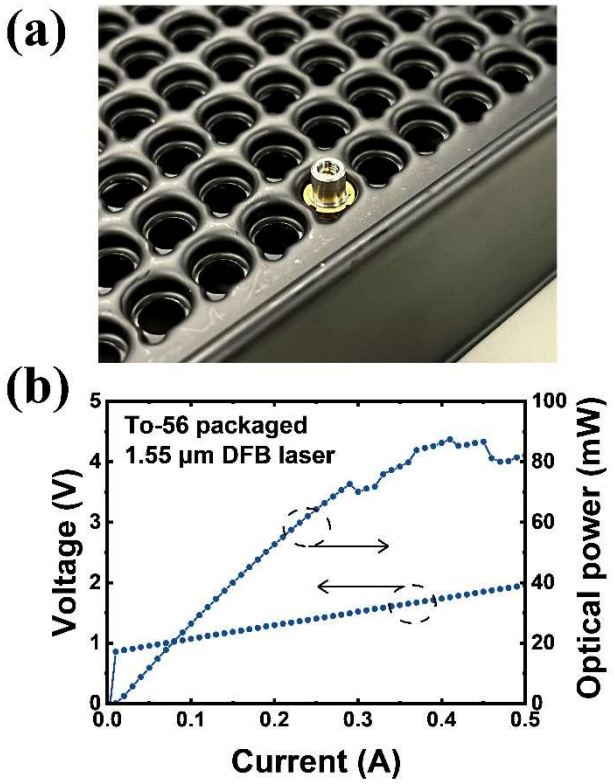

Fig. 1(a) The figure depicts a 1.55 μm BHDFB laser encapsulated using the To-56 packaging process; (b) The diagram shows the light-current-voltage characteristics of the packaged 1.55 μm BHDFB laser under room temperature conditions.

Fig. 2 displays the results of spectrogram measurements of BHDFB lasers at different temperatures. The results show that the laser can maintain its single longitudinal mode optical characteristics even in high-temperature environments. At room temperature, the peak wavelength is approximately 1551.38 nm, while at 85°C, it is 1557.24 nm. The overall SMSR values are all above 35 dB. These results demonstrate the wavelength stability of BHDFB in high-temperature environments. In addition, stable wavelengths can also assist the reception stability of LiDAR systems.

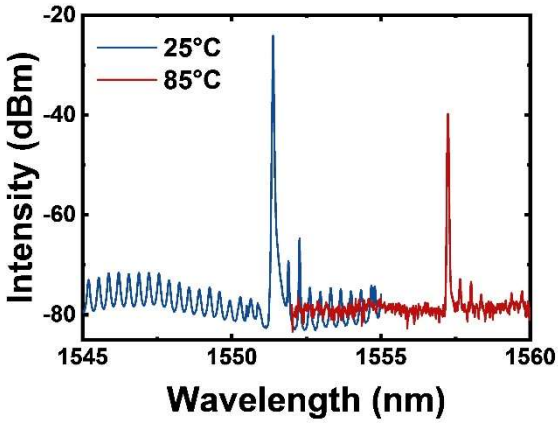

Fig. 2. The spectral analysis was measured under room temperature and 85°C with a fixed injection current of 100 mA.

THE NS-LEVEL SHORT-PULSED OPERATION FOR THE DFB LASER

In the field of LiDAR, lasers are often operated in pulsed form. Because only a portion of the fixed operation period can activate the laser, this activation ratio is known as the duty cycle, as indicated by equation (1). As a result, the laser is less susceptible to thermal accumulation and can simultaneous more optical power than in CW mode.

$$Duty\ cycle(\%) = \frac{Pulse\ width\ (\text{sec})}{Period\ (\text{sec})} \qquad (1)$$

Generally speaking, the benefits of this short-pulsed operation for EEL are that the laser has a larger area for heat dissipation, and the laser diode can achieve a larger pulse optical power. However, most pulse operation modes are based on a fixed pulse width ranging from 150 to 100 ns as a standard. We combined the laser with a commercially available pulse signal circuit board to introduce a pulse electrical signal of fewer than 100 ns. We monitored the electrical signals on the board with an oscilloscope.

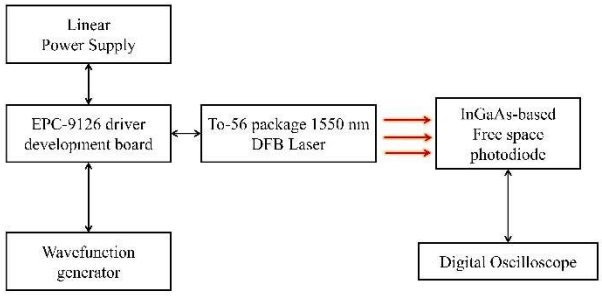

Fig. 3. Diagram of the setup for short-pulsed operation measurement.

The overall setup is shown in Fig. 3, the diagram of our short-pulsed measurement setup. We also used FSP to monitor the pulse-modulated optical signal, to confirm that the pulse width is close to the pulse width of the capacitor discharging.

The electrical signal of the packaged laser BHDFB cooperated with the short pulse driver is displayed in Fig. 4. Under the measurement conditions, the pulse of the circuit board was adjusted to 38.1 ns. The input voltage was set to 30 V. From Fig. 4(a), it can be seen that the pulse width of the circuit board's starting voltage can reach 36.4 ns. After the capacitor has completed its full charging and discharging process, the pulse width of the electrical signal is 14.5 ns. When comparing this with Fig. 4(b), which shows the pulse width of the optical signal received by the FSP, it is only 17.4 ns and is very close to the performance of the electrical signal. This demonstrates that our BHDFB laser can operate under these ns-level pulse conditions.

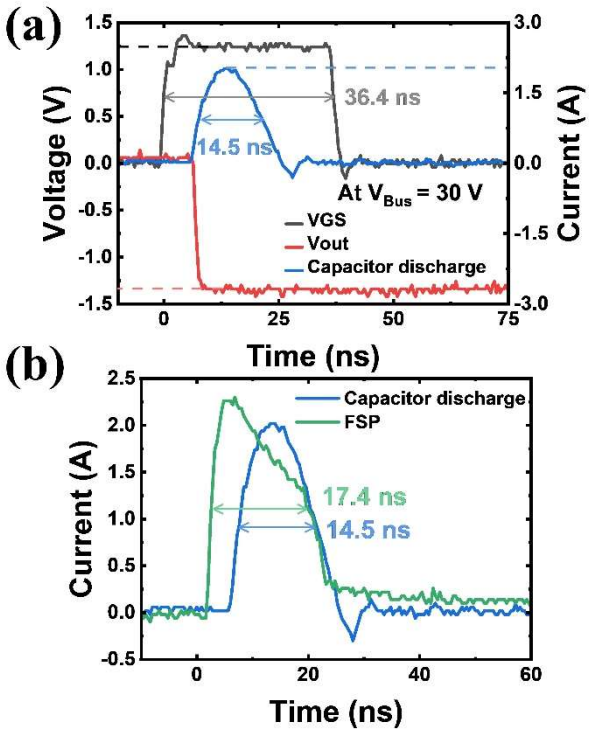

Fig. 4(a). The BHDFB laser is tested with a short-pulse circuit board, and the input/output signals of the driver are monitored using an oscilloscope; (b). The signal of the capacitor discharge is compared with the optical signal received by the FSP.

To obtain the pulse peak power of the BHDFB laser, we introduce the use of a pyroelectric sensor to measure the pulse energy of the laser during operation. The measurement setup is shown in Fig. 5. It is important to note that the laser beam area should be sufficiently concentrated on the sensor, as this can cause excessive thermal accumulation and result in a reading that is too high. To prevent this, we position the sensor as far away from the laser output as possible while stil ensuring that the pulse laser power does not reach saturation levels of the pyroelectric sensor.

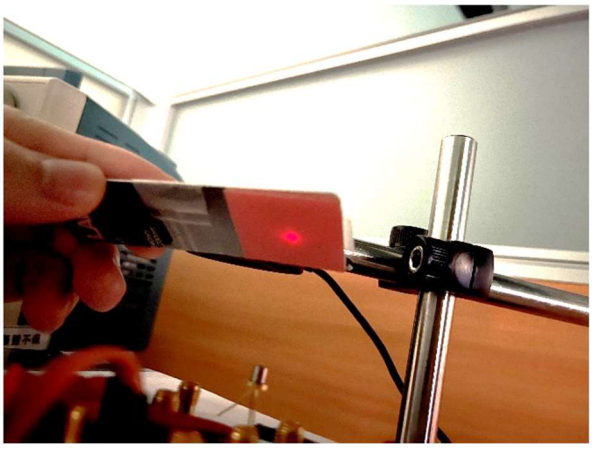

Fig. 5. Illustration of the BHDFB laser beam area using an infrared-band card.

The laser beam has an area of 22 mm^2, while the receiving area of the sensor is approximately 78.53 mm^2. Using the following equation 2:

$$Pulse\ peak\ power\ (watts) = \frac{Pulse\ energy\ (joules)}{Pulse\ width\ (\mathrm{sec})} \qquad (2)$$

From the FSP signal in the experiment, the pulse width of BHDFB is 17.4 ns. The pulse energy received by the pyroelectric sensor is about 87.4 nJ. Based on this, it can be calculated that the pulse peak power can reach 5.01 W. Compared to CW operation, pulse operation at the ns-level can increase the optical intensity by more than 50 times.

CONCLUSIONS

We have successfully designed and fabricated a 1.55 μm BHDFB laser with a low threshold current, high operating efficiency, and high wavelength stability. We also tested the possibility of operating the BHDFB laser in the nanosecond range with short pulses. As observed from the oscilloscope waveform, the optical pulses of the BHDFB laser were able to match the electrical pulses of the driver signal. Under ns-level short-pulsed operation, we can obtain excellent pulse power with an overall pulse peak power exceeding 5 W. Thus, the 1.55 μm BHDFB laser, which possesses multiple desirable features, is also highly suitable for the current automotive sensing field.

ACKNOWLEDGMENTS

This study received support from various institutions, including the National Science and Technology Council (NSTC), the National Chung-Shan Institute of Science and

Technology (NCSIST), and the National Taiwan University (NTU). The NSTC provided funding through several grant nos. 110-2224-E-992-001, 110-2622-8-A49-008-SB, 110-2622-8-002-021, 111-2221-E-002-051-MY3, 111-2119-M-002-008, 111-2119-M-002-009 and 111-2622-8-002-001. The NCSIST provided funding through grant nos. ACOM-111-6712002 and ACOM-112-6712002. NTU contributed to the study through grant nos. 109L7819, 110L2033-49, and 112L7860. Additionally, the Center for Quantum Science and Engineering also provided support for the research. The authors also thank the Semiconductor Manufacturing Lab of the Consortium of Key Technologies and the Nano-Electro-Mechanical System Research Center, NTU, for experimental and semiconductor fabrication support.

REFERENCES

[1]. Wandinger, U. (2005). Introduction to lidar. In Lidar (pp. 1-18). Springer, New York, NY.

[2]. Liu, J., Sun, Q., Fan, Z., & Jia, Y. (2018, September). TOF lidar development in autonomous vehicle. In 2018 IEEE 3rd Optoelectronics Global Conference (OGC) (pp. 185-190). IEEE.

[3]. Pfennigbauer, M., Ullrich, A., & do Carmo, J. P. (2011, June). High precision, accuracy, and resolution of 3D laser scanner employing pulsed time-of-flight measurement. In Laser Radar Technology and Applications XVI (Vol. 8037, pp. 78-84). SPIE.

[4]. Rao, S. (2017). Introduction to mmWave sensing: FMCW radars. Texas Instruments (TI) mmWave Training Series.

[5]. Schulmeister, K., Jean, M., Lund, D., & Stuck, B. E. (2019, March). Comparison of corneal injury thresholds with laser safety limits. In International Laser Safety Conference (Vol. 2019, No. 1, p. 303). Laser Institute of America.

[6]. Liu, T. H., Cheng, H. T., Yen, H. C., Yee, C. K., Yang, Y. C., Hsu, G. T., & Wu, C. H. (2022, October). High power 1.55 DFB μm laser with GHz modulation capability for low-orbit optical communication system. In 2022 28th International Semiconductor Laser Conference (ISLC) (pp. 1-2). IEEE.

ACRONYMS

FP: Fabry-Perot
DFB: Distributed feedback
BH: Buried heterostructure
ToF: Time of flight
FMCW: Frequency-modulated continuous wave
TO: Transistor Outline Packaged Laser Diodes
COB: Chip on board
CW: continuous wave
EEL: Edge-emitting laser
FSP: Free space photodiode